An Enhanced Transmission Line Method for Modelling Laminar Flow of Liquid in Pipelines

Nigel Johnston (corresponding author, d.n.johnston@bath.ac.uk)
Min Pan
Sylwester Kudzma

Department of Mechanical Engineering, University of Bath, BA2 7AY

Summary

The transmission line method (TLM) is a very efficient method for dynamic modelling of flow in pipelines, and uses delay elements to represent wave propagation. In this paper an existing TLM model is investigated and shown to have some deficiencies. An alternative technique is introduced to enhance the transient and steady state accuracy. Extremely good agreement is obtained between this new TLM and an analytical model. The model has been implemented in simulation of a number of highly dynamic systems, and has been found to be robust and reliable.

1. Introduction

Several techniques for dynamic modelling of flow and pressure of liquids in pipelines are available, ranging from simple lumped element methods (LEM) [1], to the Method of Characteristics (MOC) [2,3], the finite element method (FEM) [4], various modal approximation (MA) methods [5, 6], and the Transmission Line Method (TLM) [7, 8, 9, 10]. The TLM has been shown to be a very effective method for modelling unsteady flow and pressure in pipelines. It can model sudden transients, such as those caused by sudden closure of a valve, clearly and precisely, retaining the sharp wavefronts without the unrealistic oscillations or excessive smoothing that may occur with other methods such as the FEM or LEM. The modal frequencies of the pipeline can be captured accurately up to a very high frequency. Frequency dependent

friction can be included. TLM models can be incorporated easily into system models, and are compatible with variable timestep solvers. Furthermore TLM models are ideally suited to parallel computation because of the delays introduced between the pipe ends [11, 12].

There are some limitations to the TLM, however. It is effectively a linearized model and so the fluid properties need to be assumed to be independent of pressure, flowrate and position. For this reason cavitation and air release cannot be modelled easily, although an approximate method can be used where these effects are assumed to occur within lumped compressible volumes at the pipe ends.

For most fluid system modelling scenarios, the important features of excitation and transient responses tend to be over a fairly low frequency range, and high fidelity up to a very high bandwidth is not necessary. Simpler pipeline models such as lumped element models can be used. However in some situations rapid dynamics, high bandwidth and high fidelity are necessary. Examples might include anti-lock braking systems, fuel injection systems, and fast-switching 'digital' hydraulic systems [13, 14].

A TLM model was presented by Johnston [10]. In this model some of the deficiencies of previous TLM models were addressed, particularly with respect to frequency-dependent friction. However it still had some inherent inaccuracies. An improved, alternative method is presented in this paper. The inaccuracies in the previous model are explained, the new model is developed and the parameter optimization technique is explained, and some results from the model are compared with analytical results.

2. Analytical model and block diagram representation

Flow and pressure in a pipeline can be represented by the transmission matrix [15], shown in non-dimensional form in equation (1).

$$\begin{pmatrix} P_1 \\ Q_1 Z_C \end{pmatrix} = \begin{pmatrix} t_{11} & t_{12} \\ t_{21} & t_{22} \end{pmatrix} \begin{pmatrix} P_2 \\ Q_2 Z_C \end{pmatrix} = \begin{pmatrix} \cos\left(\frac{\omega L}{c}\sqrt{N}\right) & -j\sqrt{N}\sin\left(\frac{\omega L}{c}\sqrt{N}\right) \\ \frac{j}{\sqrt{N}}\sin\left(\frac{\omega L}{c}\sqrt{N}\right) & -\cos\left(\frac{\omega L}{c}\sqrt{N}\right) \end{pmatrix} \begin{pmatrix} P_2 \\ Q_2 Z_C \end{pmatrix} \quad (1)$$

$$Z_C = \frac{\rho c}{A} \quad (2)$$

This assumes that the properties are independent of pressure, temperature and position along the length of pipe. N is a frequency dependent function that depends on the type of friction model that is used. A commonly used expression is based on the "two-dimensional viscous compressible" model [16] in which the effects of frequency-dependent radial variations in velocity are included but thermal effects are neglected. This model is generally suitable for liquid flow in small diameter lines ($r << \lambda$), and is given by equations (3)-(5).

$$N = -\frac{J_0(z)}{J_2(z)} = \frac{1}{1 - \frac{2}{z}\frac{J_1(z)}{J_0(z)}} \quad (3)$$

where $z = j\sqrt{j\alpha}$ (4)

α is the non-dimensional frequency, $\alpha = \frac{r^2\omega}{\nu}$ (5)

Equations (1) to (5) can be implemented readily in the frequency domain. However they are more difficult to transform to and implement in the time domain and approximations are generally needed. The TLM is a method to approximate these equations in the time domain.

The TLM model must satisfy several requirements and model the following effects correctly:

- Steady state pressure drop;
- Capacitance and inertance;
- Mass or flow continuity;
- Wave delay, decay and dispersion.

In the absence of friction ($N=1$), the TLM is extremely simple and can be implemented using delays and algebraic equations. When friction is included, it becomes more complicated and approximations are needed, largely because N is complex and frequency dependent. Krus et al [8] and Johnston [9, 10] represented the equations by a block diagram similar to that shown in figure 1, where

$$P_1 = C_1 + Z_C Q_1 \tag{6}$$

$$P_2 = C_2 + Z_C Q_2 \tag{7}$$

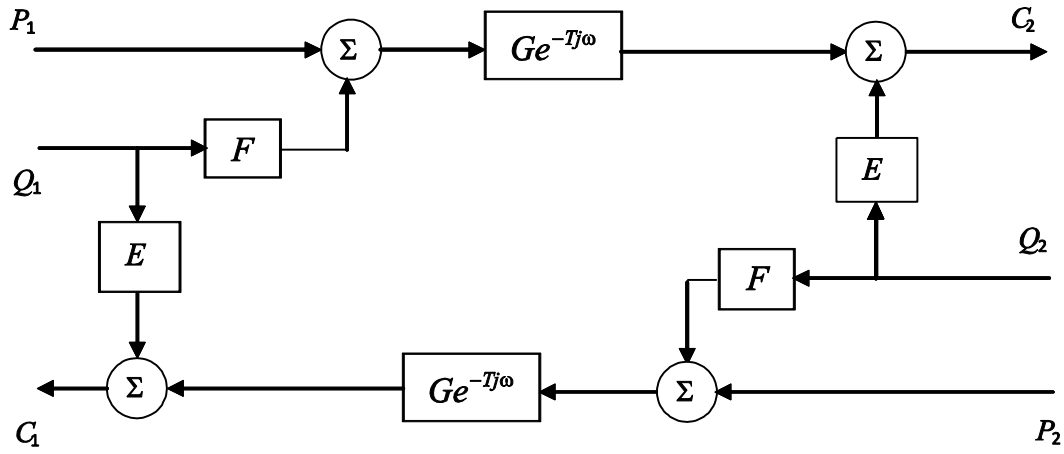

Figure 1 Block diagram for transmission line model [8]

The transmission matrix terms for the block diagram shown in figure 1 can be determined by setting different boundary conditions. By setting P_2 to zero the relationship between P_1 and Q_2 gives t_{12}^*, and the relationship between Q_1 and Q_2

gives t_{22}^*. Similarly by setting Q_2 to zero, t_{11}^* and t_{21}^* can be found. Consequently the transmission matrix terms are given by equations (8) – (11).

$$t_{11}^* = \frac{(E + Z_C)G^{-1}e^{j\omega T} + FGe^{-j\omega T}}{(E + Z_C + F)} \tag{8}$$

$$t_{12}^* = \frac{(E + Z_C)^2 G^{-1}e^{j\omega T} - F^2 Ge^{-j\omega T}}{Z_C(E + Z_C + F)} \tag{9}$$

$$t_{21}^* = \frac{(Ge^{-j\omega T} - G^{-1}e^{j\omega T})Z_C}{E + Z_C + F} \tag{10}$$

$$t_{22}^* = -t_{11}^* \tag{11}$$

The block diagram in figure 1 is an exact representation of the analytical transmission matrix, equation (1), if the terms are as follows [8].

$$E = Z_C(\sqrt{N} - 1) \tag{12}$$

$$F = Z_C\sqrt{N} \tag{13}$$

$$G = e^{-j\omega T(\sqrt{N}-1)} \tag{14}$$

3. Previous Transmission Line Model

Krus *et al*. [8] derived a model which was enhanced by Johnston [10] to include frequency-dependent friction, using equations (15) – (20).

$$E(j\alpha) = \frac{8\beta\rho c}{A(\kappa\beta j\alpha + 1)} \tag{15}$$

$$Z_C = \frac{\rho c}{A}\left(1 + \kappa\left[1 - e^{-4\beta}\right] + 2\sum_{i=1}^{k}\frac{m_i}{n_i} - 4\beta\right) \tag{16}$$

$$F = Z_C \tag{17}$$

$$G(j\alpha)=\frac{\kappa\beta j\alpha e^{-4\beta}+1}{\kappa\beta j\alpha+1}\frac{1}{1+2\beta\sum_{i=1}^{k}\left(\frac{m_i j\alpha}{n_i+j\alpha}\right)} \tag{18}$$

β is the dissipation number, $\beta=\frac{\nu L}{cr^2}=\frac{\nu T}{r^2}$. (19)

κ is an empirical coefficient, $\kappa=1.25$. (20)

The characteristic impedance Z_C was adjusted using the correction in parentheses in equation (16) to compensate for the effect of the frequency-dependent friction on the effective capacitance.

Johnston [10] showed that this model gave reasonably accurate results in response to a step change in pressure or flow, but gave a slight overestimate of the magnitude of the pressure pulsation immediately following a step change in flow and a small error in the shape of the pulsations. The decay of the pulsations was predicted very well.

To determine the reasons for the inaccuracies in the basic TLM results, the transmission matrix obtained using the approximate equations in the frequency domain was investigated. Figure 2 shows the analytical (equations (1) – (5)) and approximated (equations (8) – (11) and (15) – (20)) transmission matrices, for two different dissipation numbers, $\beta=0.01$ and 0.1. The agreement is reasonably good but there are noticeable differences.

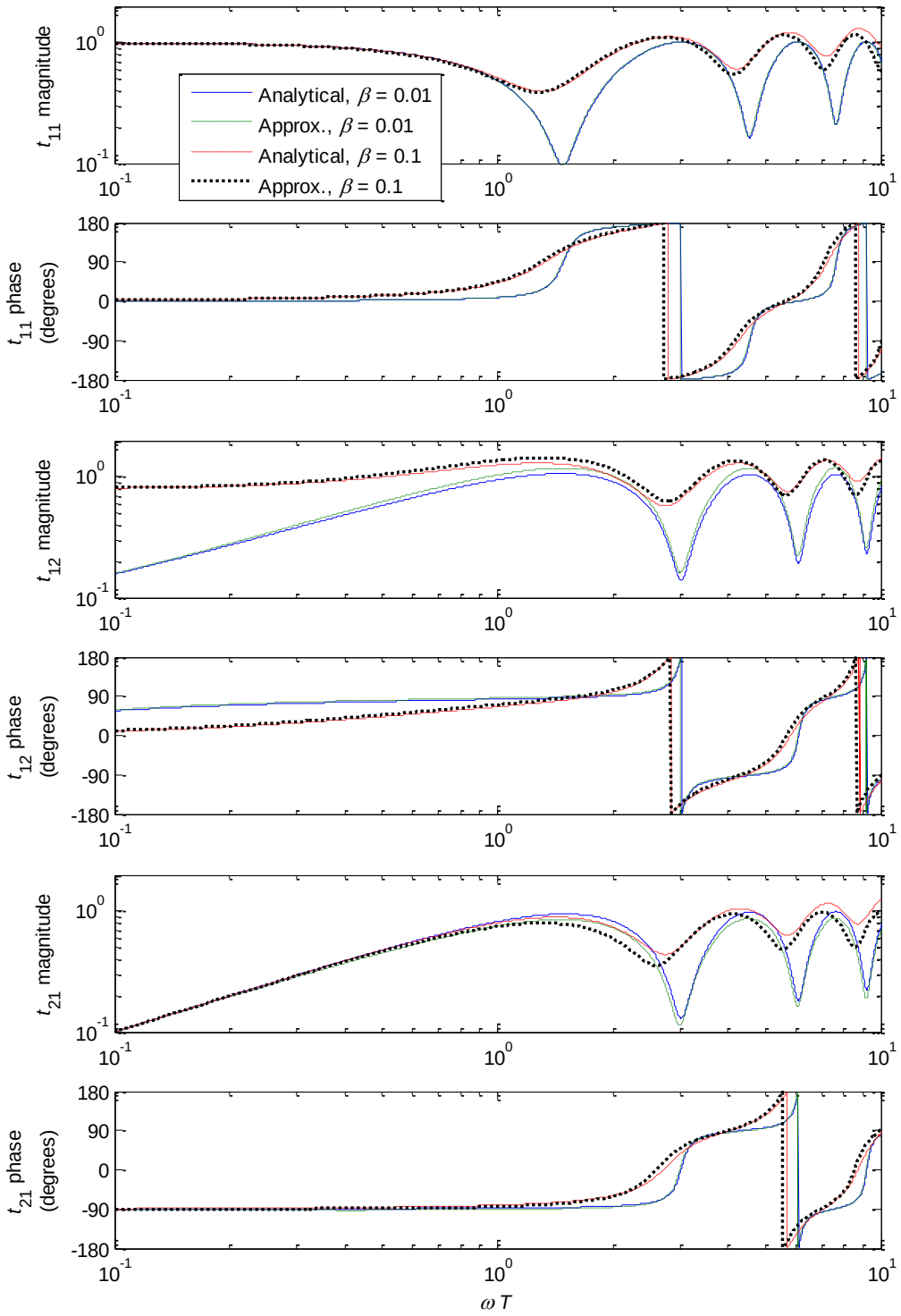

Figure 2 Transmission Matrix for previous TLM model

3. New Transmission Line Method

Because of the inaccuracies in the previous TLM, an alternative configuration was investigated in which $E(j\omega)$ and $G(j\omega)$ are represented using separate weighting functions, equations (21) and (22).

$$E(j\omega) = Z_C \sum_{i=1}^{k} \frac{m_{Ei}}{n_i + j\omega T} \tag{21}$$

$$G(j\omega) = 1 - \sum_{i=1}^{k} \frac{m_{Gi}\, j\omega T}{n_i + j\omega T} \tag{22}$$

$F(j\omega)$ is scaled from $E(j\omega)$ in order to maintain the correct steady state pressure drop, according to the constraint given by equation (23) [8, 10]

$$F(0) - E(0) = Z_C(1 - 8\beta) \tag{23}$$

This constraint is satisfied by equations (24) and (25).

$$F(j\omega) = Z_C + bE(j\omega) \tag{24}$$

$$b = 1 - \frac{8\beta}{\sum_{i=1}^{k} \frac{m_{Ei}}{n_i}} \tag{25}$$

Other weighting series were tried for $F(j\omega)$, and the most general was given by equation (26), with an independent set of weights m_{Fi}.

$$F(j\omega) = Z_C \left(1 + \sum_{i=1}^{k} \frac{m_{Fi}}{n_i + j\omega T} \right) \tag{26}$$

However this required extra optimisation effort, an extra table of weights, and extra computation. The approach given by equations (24) and (25) was found to give no significant loss of accuracy, and was more efficient and convenient.

Best results were obtained by also adjusting the time delay T' by a factor τ as in equation (27).

$$T' = \frac{\tau L}{c} \tag{27}$$

2.1 Optimisation

The weighting functions were optimised to minimise the error between the analytical equations and the TLM model. The success of this was strongly dependent on the object function to be minimised, and on the optimisation parameter set. The optimisation parameter vector was $[m_{E1} \ldots m_{Ek}\, m_{G1} \ldots m_{Gk}\, \tau]$, and the parameters were limited to positive values. It was found to be difficult to obtain reliable results if the n_i terms were included as optimisation parameters, so these were set manually. The success of the optimisation was strongly dependent on the values of n_i. The following series was found to give good results.

$$n_1 = \frac{0.3}{1+3\beta},\ n_{i+1} = 3n_i \tag{28}$$

Several approaches were considered, including:

1. Optimising the response in the time domain for simple boundary conditions;
2. Optimising the weighting functions $E(j\omega)$, $F(j\omega)$ and $G(j\omega)$ (equations 21, 22, 24, 25) to their analytical counterparts (equations 12-14) in the frequency domain.
3. Optimising the transmission matrix terms in the frequency domain;

Approach (1) was rejected because it would be extremely computationally intensive and may be subject to numerical integration errors. Approach (2) was found to give good agreement between the weighting functions and their analytical counterparts, but gave less reliable overall results with steady state errors. Most success was obtained by approach (3), minimising the error in the transmission matrix

terms in the frequency domain. In doing so, the weighting between the transmission matrix terms, and the frequency range and weighting, needed to be selected carefully in order to emphasise the important features of the transmission matrix. It was also necessary to ensure that the object function was sensitive to all of the parameters being optimised in order to provide clearly defined minima and good convergence. The object function given by equations (29)-(31) was found to give good results. It was designed to emphasize the low frequency accuracy of the $t_{12}(\omega)$ and $t_{21}(\omega)$ terms. It was found not to be beneficial to include $t_{11}(\omega)$ or $t_{22}(\omega)$ in the object function.

$$\varepsilon = \sum_{0.01 \le \omega T \le n_k} \frac{\left|t_{12}(\omega) - t_{12}^*(\omega)\right|^2}{\omega T} + \sum_{0.01 \le \omega T \le n_k} \frac{\left|t_{21}(\omega) - t_{21}^*(\omega)\right|^2}{(\omega T)^2} + \varepsilon_E + \varepsilon_G \tag{29}$$

$$\varepsilon_E = \sum_{i=3}^{7} \left[\max\left(0, m_{Ei} - 3m_{Ei-1}\right)\right]^2 \tag{30}$$

$$\varepsilon_G = 10\left[\max\left(0, \sum_{i=1}^{7}(m_{Gi}) - 1\right)\right]^2 \tag{31}$$

Here $t_{12}(\omega)$ and $t_{21}(\omega)$ represent theoretical values (equations 1-5), and $t_{12}^*(\omega)$ and $t_{21}^*(\omega)$ modelled values (using equations 8-11 and 15-20), at frequency ω. The summation in equation (28) was done for frequency points spaced in a geometric series with 50 points per decade, for $0.01 \le \omega T \le n_k$. The additional error terms ε_E and ε_G are included to act as 'soft' constraints, and are zero if the constraints are not violated but increase according to the amount by which the constraints are violated. ε_E limits the 3rd – 7th terms in the m_{Ei} series to a maximum of three times the previous term, to avoid excessive higher order terms and smooth the variation in the m_{Ei} series. ε_G limits the sum of the terms in the m_{Gi} series to a maximum of 1. This

ensures that the output of the *G* filter is of the same sign as the input during a rapid transient. Without this constraint, a step input may result in very short duration, unphysical spikes in the response. Similar spikes were observed by Johnston [10], specifically in figure 4 of that paper.

The optimization was done separately for numbers of terms *k* from 3 to 7, and for values of β from 10^{-6} to 1 with 8 steps per decade.

The optimisation was done using a simple Newton-Raphson approach. There may be several local minima and this approach may not find the global minimum, but this is not necessarily a problem provided that a sufficiently good approximation is obtained. However in most cases the results were found to be independent of the starting conditions for the iterations, which suggests that there may be a single minimum for the object function and no other local minima. The exception to this was for $\beta > 0.1$ where different solutions were obtained for different starting values. In these cases the converged weighting values were used as the starting point for the iteration at the next value of β, in order to try to obtain a reasonably smooth and gradual variation of values with β. A smooth, gradual variation helps to improve the accuracy of the model when interpolation is used to obtain the weighting terms for other values of β.

2.2 Optimisation results

The coefficients for $k = 6$ are listed in appendix 2, tables 3-4. Analytical and approximated transmission matrices are shown in figure 3 for two examples, $\beta = 0.01$ and 0.1, using six terms ($k = 6$). The agreement is extremely good and the analytical and approximate lines overlay each other closely. The optimisation was less successful for $\beta > 0.5$.

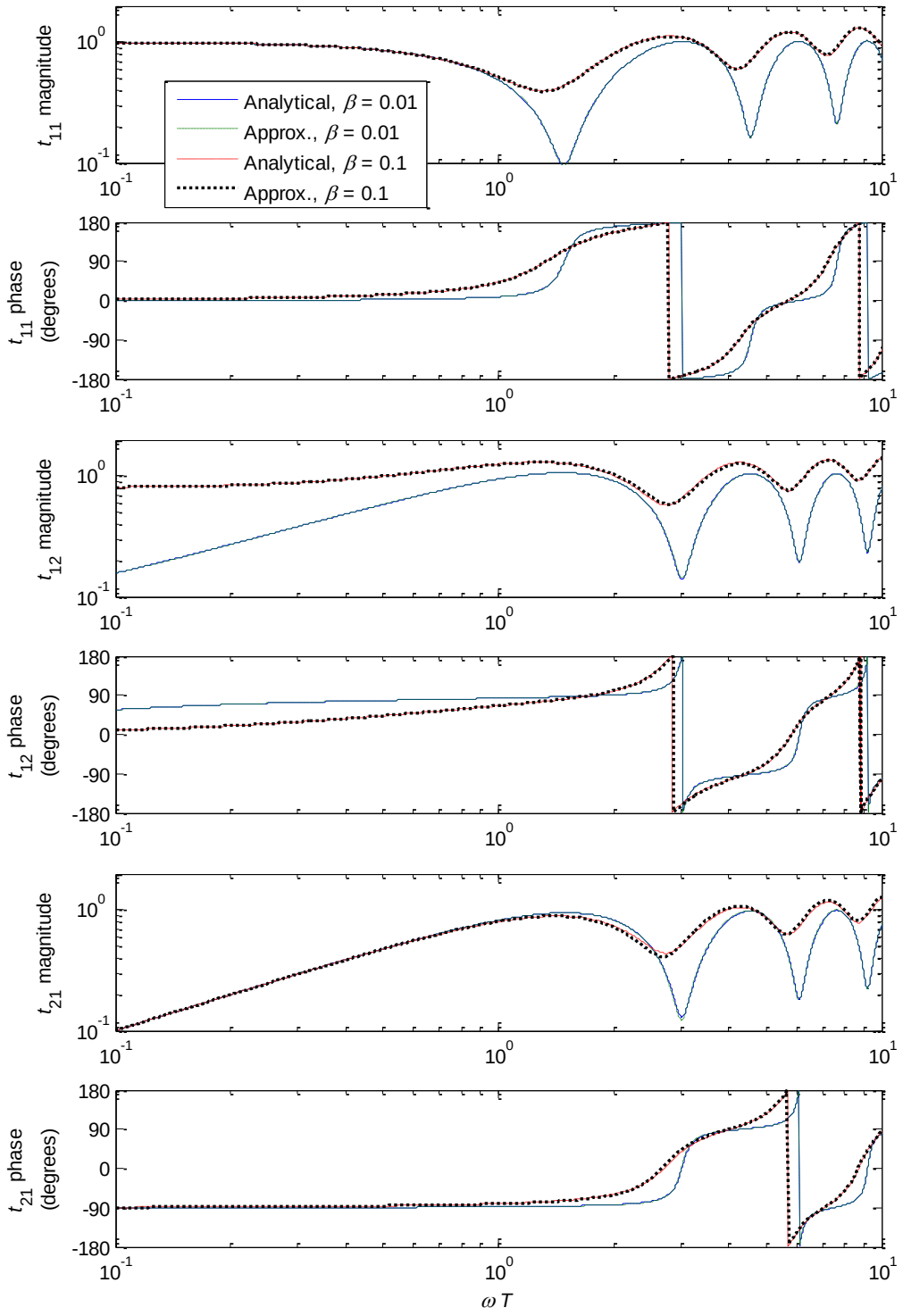

Figure 3 Transmission matrix for new TLM

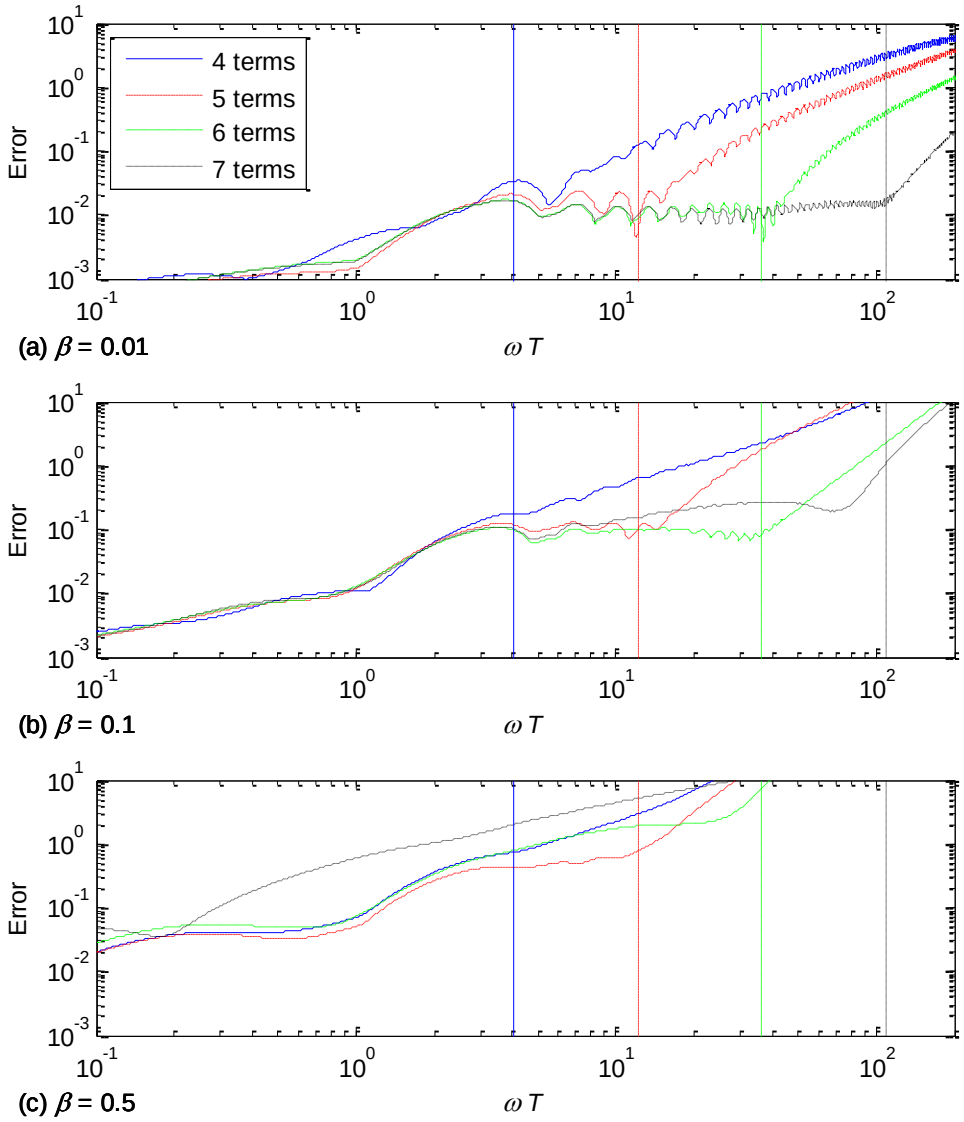

Figure 4 Error in transfer matrix (vertical lines are at $\omega T = n_k$ which is the upper limit of the optimization band)

Figure 4 shows the error ε, which is defined by equation (32).

$$\varepsilon = \left|t_{11} - t_{11}^*\right| + \left|t_{12} - t_{12}^*\right| + \left|t_{21} - t_{21}^*\right| \tag{32}$$

The error is generally less than 10^{-2} within the optimization band, but rises at higher frequencies. The error increases with β. It was not possible to obtain a good optimisation for $\beta \geq 0.3$ with 7 terms, but 6 or fewer terms are likely to be sufficient.

Linear interpolation can be used to obtain the weighting values for values of β between the optimised values. As the weighting functions are approximately proportional to $\sqrt{\beta}$, the accuracy was found to be very slightly improved if the interpolation is done relative to $\sqrt{\beta}$. For $\beta < 10^{-6}$ the parameters m_{Ei} and m_{Gi} can be scaled proportionally to $\sqrt{\beta}$ with sufficient accuracy.

The weighting functions are shown in figure 5 for β = 0.01 and 0.1. Over this frequency range there are clear differences between the theoretical and approximate terms, particularly for the phase of E and F. The accuracy of the individual terms is less good than that of the overall transmission matrix, but that is not necessarily a problem as they are only internal components of the model.

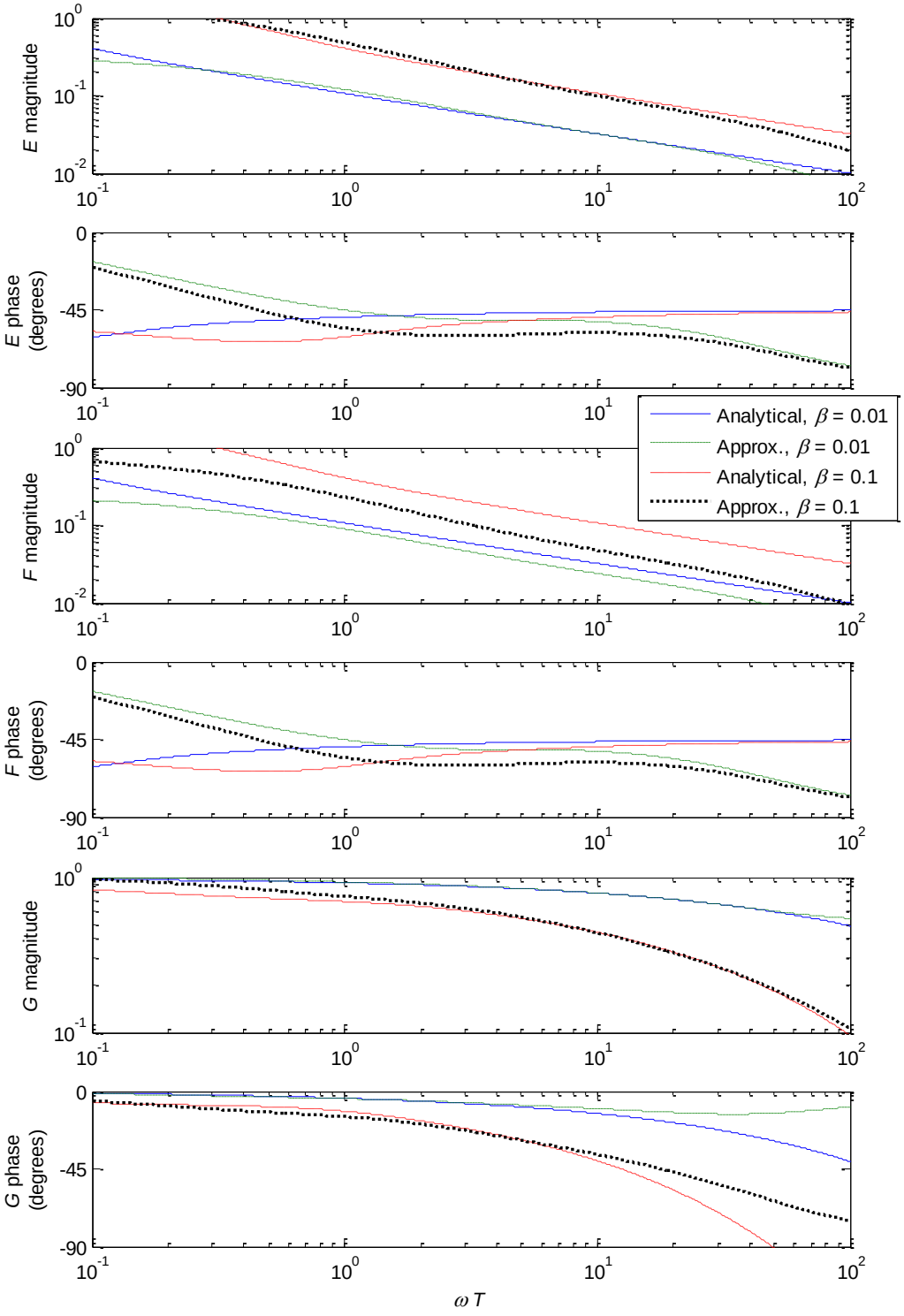

Figure 5 Weighting functions for new TLM

3.2 Time domain results

The results were compared with step response solutions obtained using an inverse discrete Fourier transform of the transmission matrix [4]. In this paper, this is called the 'analytical' solution, although strictly speaking there are some very small errors in this approach, caused by:

- Truncation of the harmonic series. Provided that sufficient harmonics are taken, this should be negligible.
- Discrete harmonic points. In effect the excitation is a squarewave, that is, a series of steps and not a single step. It is necessary that the time between subsequent steps is long enough for the transient to decay to negligible levels before the next transient occur. If not, the transient response will be distorted. This is most likely to be a problem for low damping levels where the decay time is long.

These conditions can be satisfied by using a very large number of frequency points. In the cases presented here 2^{18} points were found to be sufficient.

Figure 6 shows predicted pressure responses, for a step change in flow at the upstream end and a fixed pressure at the downstream end, for different numbers of terms *k*. The accuracy deteriorates as the number of terms *k* is reduced. For six and seven terms, the response is indistinguishable from the analytical result. In all cases the correct steady state pressure drop is predicted.

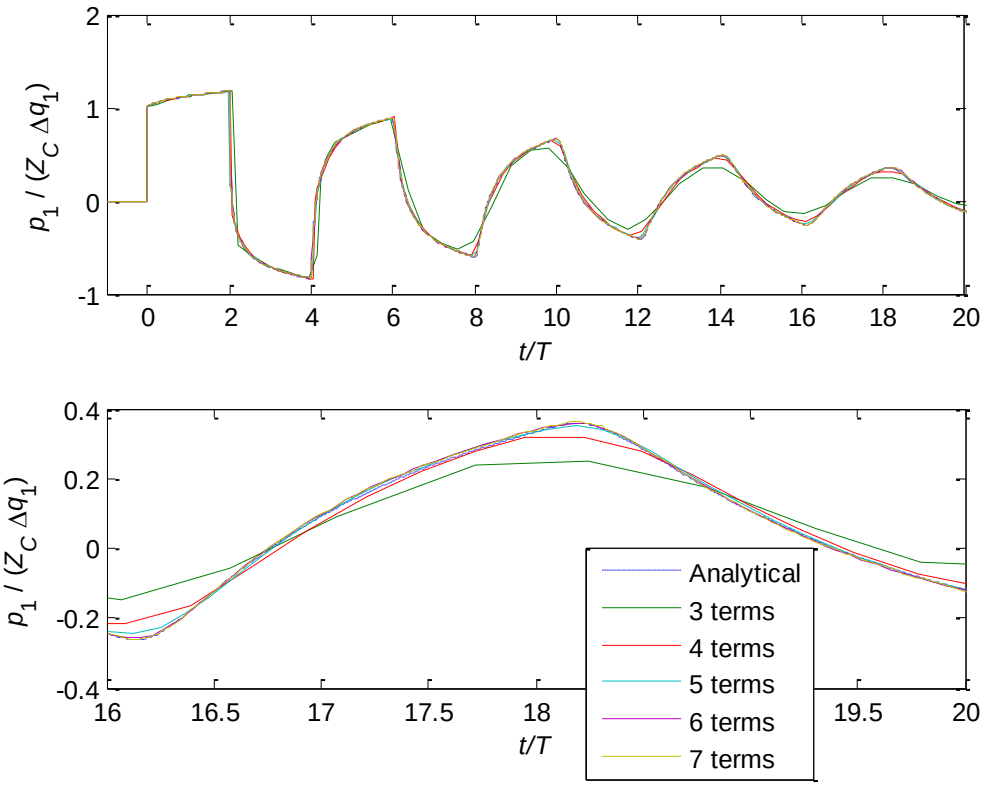

Figure 6 Pressure response to a step change in upstream flow with a fixed downstream pressure, for different numbers of terms, $\beta = 0.01$. Upper plot shows the early part of the transient, lower plot shows a small part of the decaying oscillation

Little improvement was obtained by using more than six terms, and subsequent results are shown using six terms.

Predicted step responses are shown in figure 7, for a step change in flow at the upstream end and a fixed pressure at the downstream end. The agreement with the analytical response is extremely good (the lines overlay each other), and the correct steady state pressure drop is predicted.

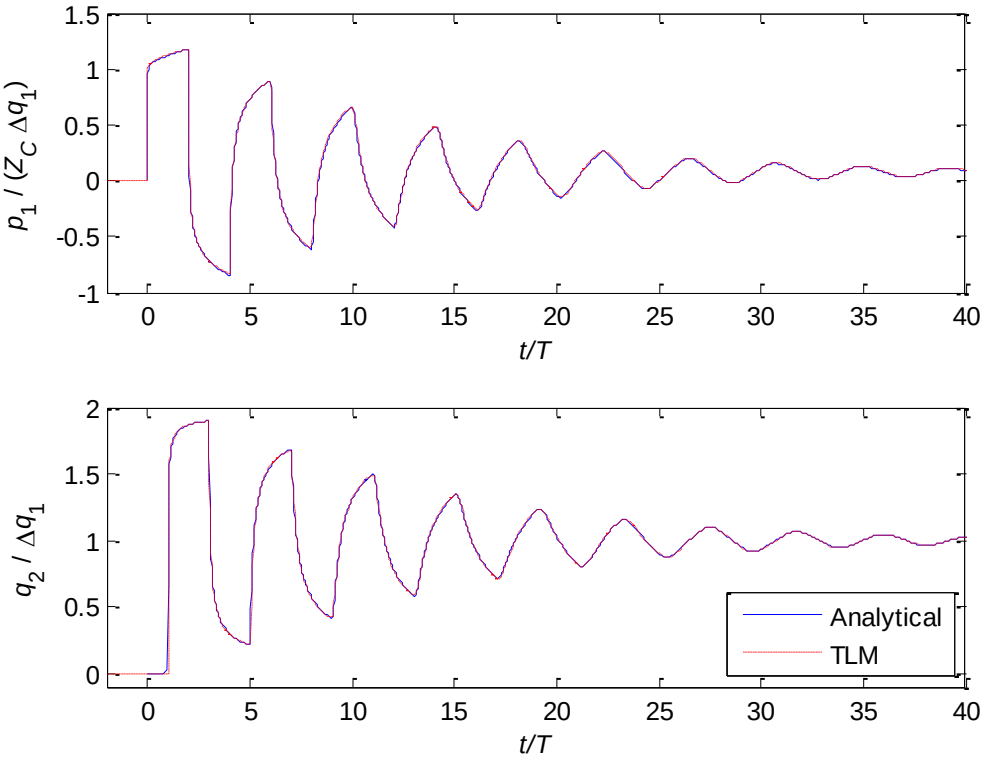

(a) $\beta = 0.01$

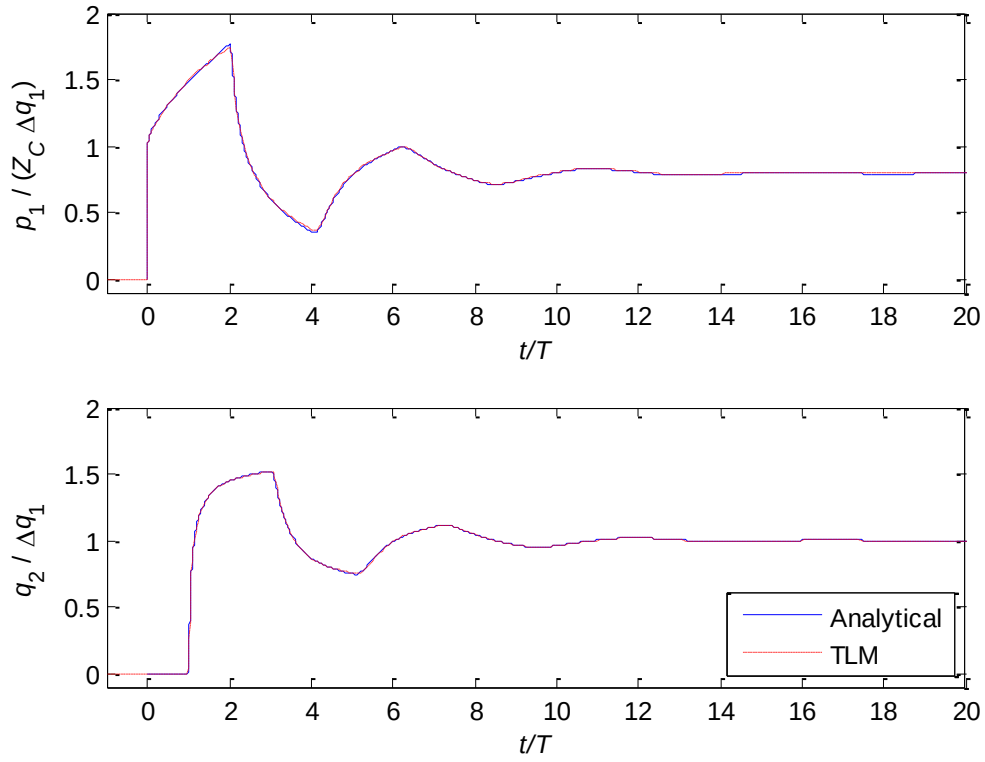

(b) $\beta = 0.1$

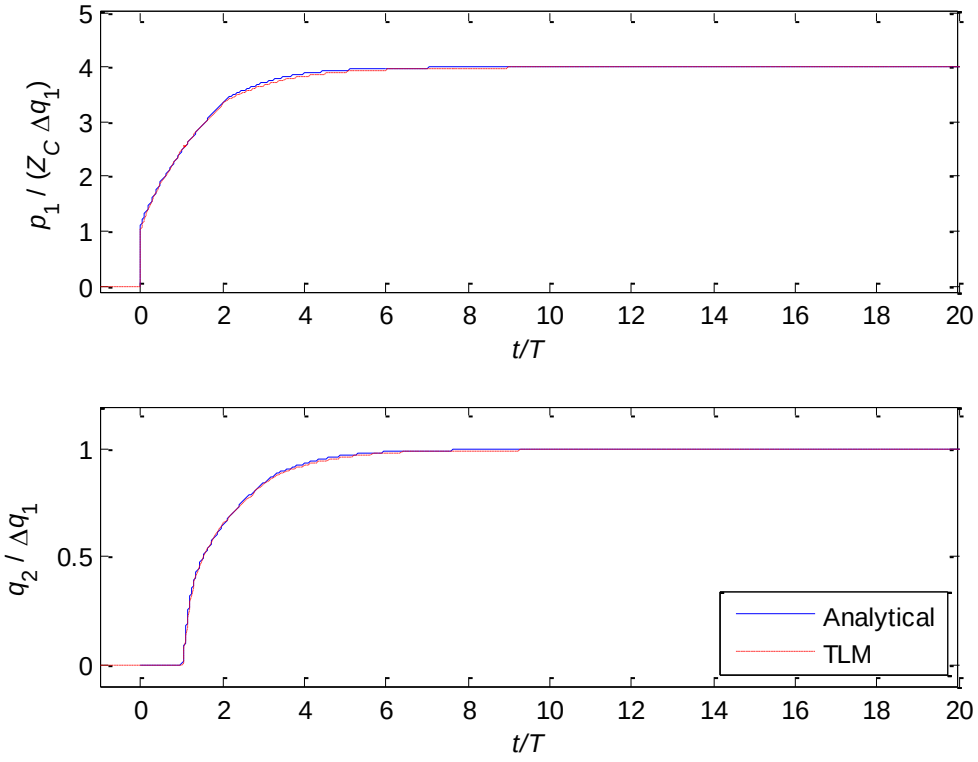

(c) $\beta = 0.5$

Figure 7 Response to a step change in upstream flow with a fixed downstream pressure

Figure 8 shows a comparison between the normalized initial pressure peaks following a flow step for a range of values of β, for similar conditions to figure 5. The axes are normalized such that the analytical curve is independent of β and identical to that of an anechoic line until the point at which the downward step occurs due to the first reflection. It can be seen that the magnitude and shape of the TLM model predictions match the analytical curve very closely, to within 1% at all times. In all cases the agreement is better than for the previous model [10].

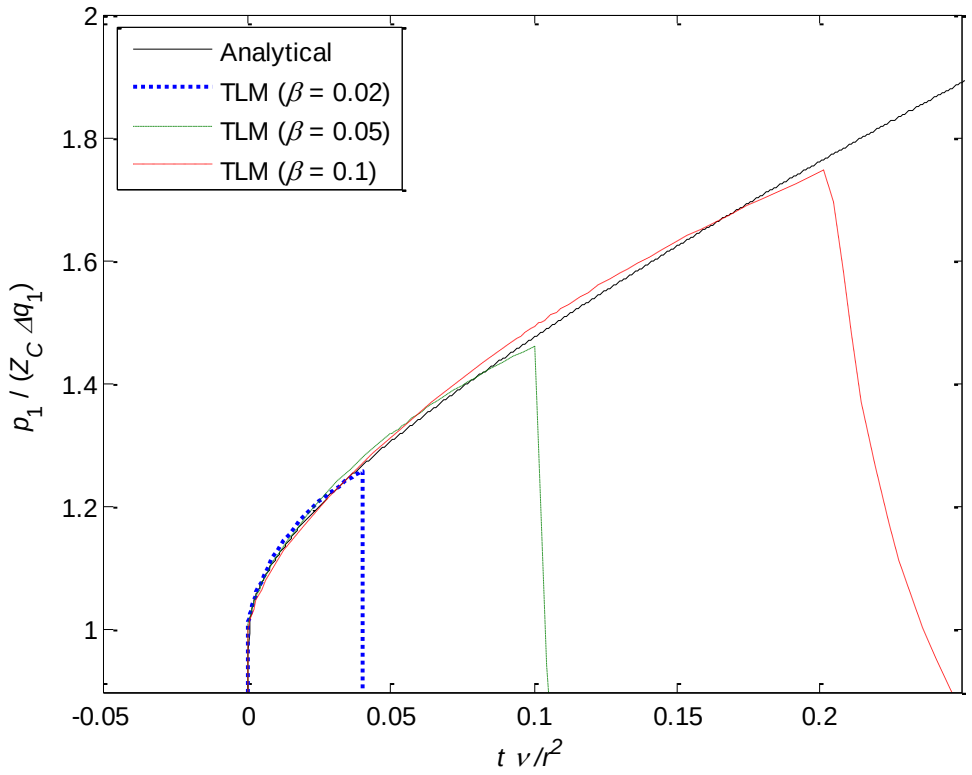

Figure 8 Pressure response to a step change in flow (comparison with analytical response of a very long or anechoic line)

Figure 9 shows the normalized predicted pressure for a closed-ended line with a smooth sinusoidal pulse of flow at one end of period $t/T = 5$. A smooth pulse was used so that the steady state pressure rise could be seen more clearly without being swamped by high frequency pulsations. The steady state pressure and the shape of the transient are captured very accurately and are almost indistinguishable from the analytical responses.

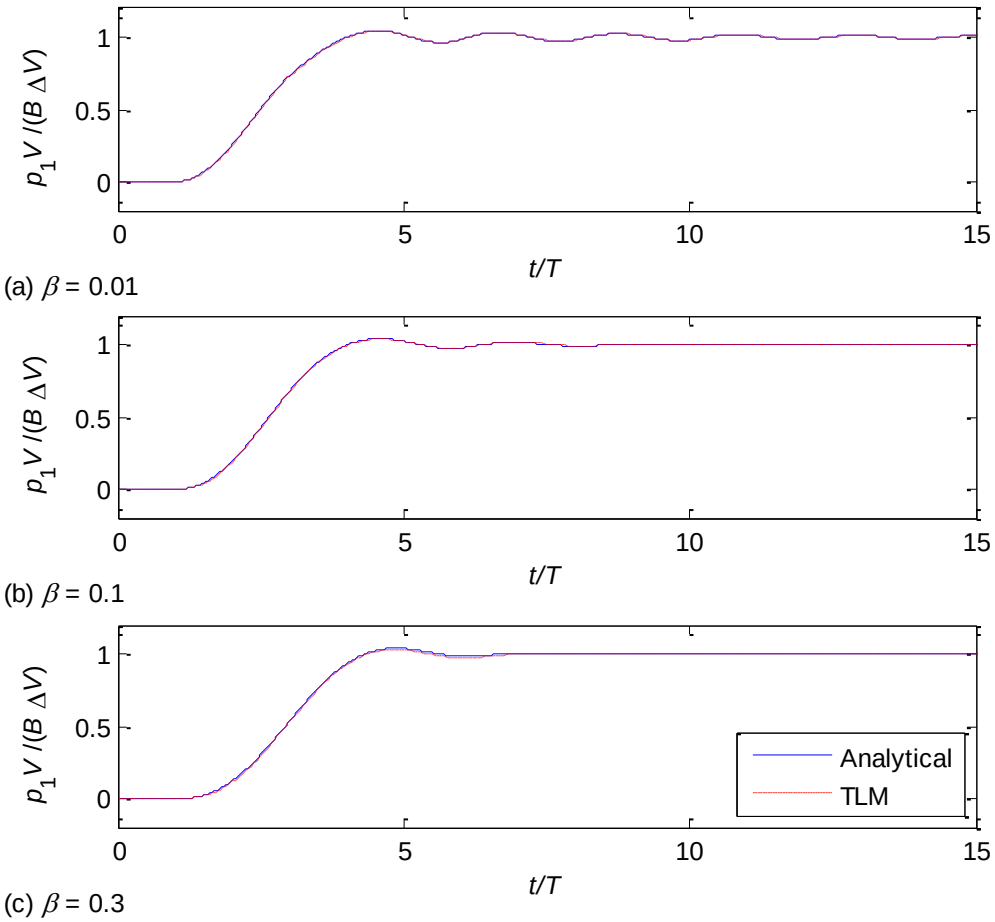

Figure 9 Predicted pressure (non-dimensionalised) for a flow pulse at one end with the other end blocked

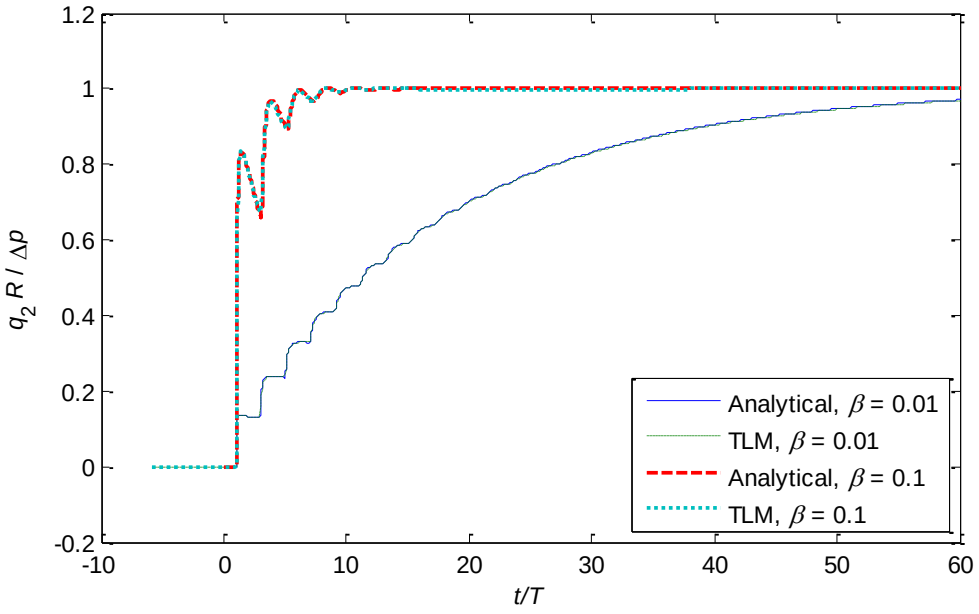

Figure 10 Predicted flowrate (non-dimensionalised) in response to a step change in pressure, with a fixed pressure at the other end

Figure 10 shows the response to a step change in upstream pressure Δp, with a constant downstream pressure. The response of the new model agrees extremely well with the analytical response. The steady state flowrate is predicted very accurately in both cases.

4. Experimental Results

The TLM has been used to model a 'switched reactance' hydraulic system [14, 17] and simulation results have been compared with experimental measurements.

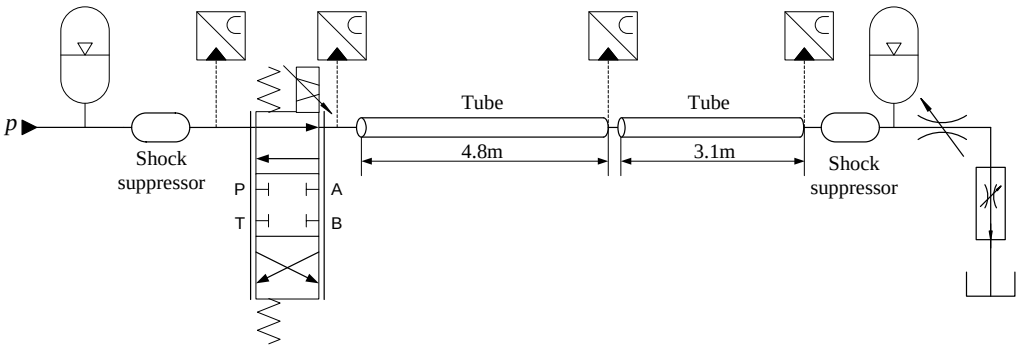

Figure 11 Simplified Circuit Diagram

The test rig is shown in figure 11. The proportional valve was a Parker Hannifin DF*plus* D1FP. In the results shown here, pulsations were generated by switching the valve between 21% opening and 38% opening using a 5 Hz square wave. This was a simplified mode of operation which was done for development of the test rig and system model; to operate as a 'switched reactance' system two supply lines are needed [14, 17]. Simulation and experimental parameters are listed in table 1. More details are given in [17].

Table 1 Parameters for the simulations and experiments

Density ρ	870 kg/m^3
Viscosity υ	32 cSt
Switching frequency	5 Hz
Inertance tube length	7.9 m
Inertance tube diameter	7 mm
Speed of sound c	1293 m/s
Oil temperature	40 °C
Supply pressure	55 bar
Valve pressure/flow characteristic	18 L/min at 10 bar pressure drop, 100% opening
Mean flowrate	7 L/min
Downstream pressure	46.6 bar

The shock suppressor downstream of the tube was modelled as a capacitance of 0.01L/bar, which resulted in an effectively constant downstream pressure. The measured valve spool position was used in the simulation. Experimental and simulated results are shown in figure 12, showing the measured valve spool position and the pressures measured upstream of the 4.8m tube and midstream between the 4.8m and 3.1m tubes. Agreement between measured and simulated pressures is good. For the mid-stream pressure, figure 12(c), the decaying pulsations due to wave effects can clearly be seen in the experimental and simulated results. The amplitude, decay rate and shape of the pulsations in the mid-stream pressure are predicted quite well.

The speed of sound was tuned to give the best agreement as it depends on the effective adiabatic tangent bulk modulus, which in practice is difficult to determine by measurement or from manufacturer's data. It might be possible to improve the agreement slightly by tuning the viscosity as well.

The TLM model proved to be very effective in this situation and enabled an efficient and robust system model.

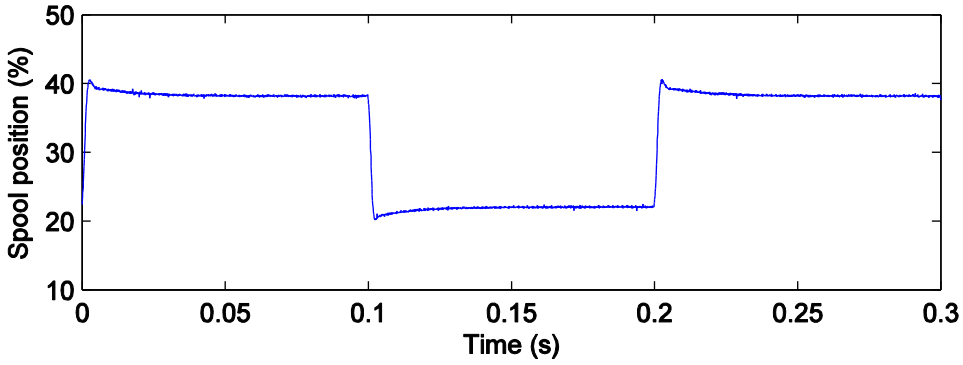

(a) Valve spool position

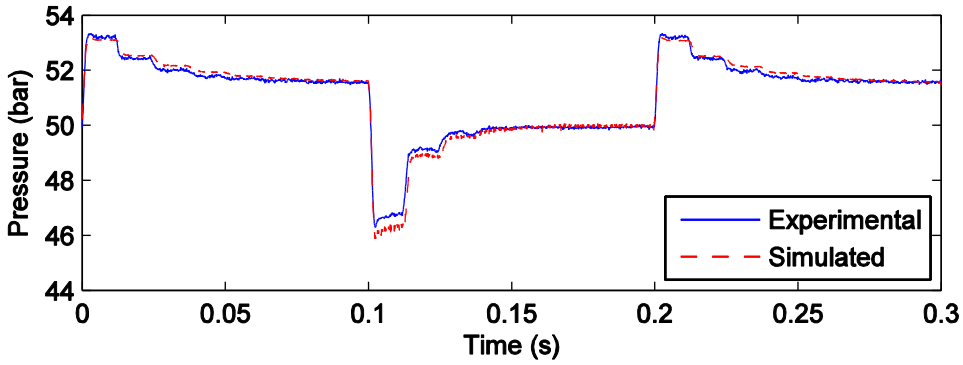

(b) Upstream pressure

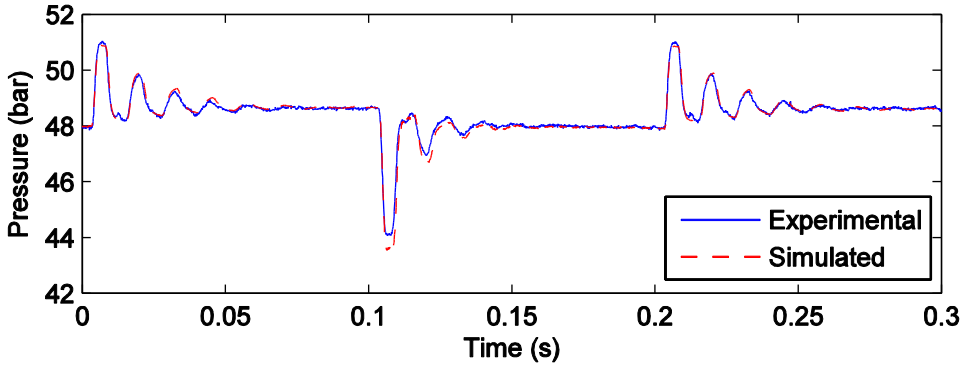

(c) Mid-stream pressure

Figure 12 Experimental and simulated pressures

5. Discussion

In a previous paper [10], a TLM model was proposed. The model has been found to give errors in the effective inertance, in the step response amplitude and shape, and in the frequency response.

A new TLM model has been proposed in this paper. This is shown to be significantly more accurate than the previous model. However it has some slight disadvantages. Firstly it may require a larger number of weighting functions than the previous model, although this depends on the required bandwidth. Secondly, the weighting values depend on the damping constant β so lookup tables are needed, whereas in the basic model the same weighting values could be used regardless of the value of β. In many situations the previous model may be sufficiently accurate. A summary and comparison of the two models is given in table 2.

Table 2 Summary of models

	Previous TLM (Johnston [10])	New TLM
Accuracy and bandwidth	Reasonably good accuracy but some error in magnitude and shape of	Very good accuracy from

	transient. Unlimited bandwidth, dependent on number of terms *k*.	steady state up to $\omega T \le n_k$. This depends on number of terms *k*.
Number of state variables	14 state variables if $k = 4$. Generally (2* *k* + 2) state variables.	24 state variables if $k = 6$. Generally 4* *k* state variables.
Stability	Good provided that suitable numerical solver is used, and that modified *G* terms (model 2 or 3) are implemented. Model 1 for *G* may be inherently unstable at high damping levels.	Good, provided that suitable numerical solver is used.
Suitability	Use when high accuracy not essential.	Use when high accuracy is needed, at the expense of slightly more complexity.
Range of β	Reasonably good results for $0 \le \beta < 0.3$	Very good results for $0 \le \beta < 0.5$

Comparison of the computational speed of the two models is difficult because it depends on many factors including boundary conditions, excitation bandwidth, required bandwidth, number of terms *k*, method of implementation and numerical solver type. Using Matlab Simulink, the new model has been found to take between one and two times longer to run than the previous model in most cases, provided that the numerical solver and the number of terms *k* are chosen appropriately in both models.

The parameters in the model have been optimized for $10^{-6} \le \beta \le 1$, although the accuracy deteriorates severely for $\beta > 0.5$. For $\beta < 10^{-6}$ the parameters m_{Ei} and m_{Gi} can be scaled proportionally to $\sqrt{\beta}$ with sufficient accuracy. However for β less than about 10^{-4}, the effect of friction in the pipeline may be unimportant and damping in adjoining components is likely to be more significant. A very simple undamped model may be adequate in this situation.

The model may not be suitable for $\beta > 0.5$, which may occur for very long lines with small diameter and high viscosity. Wave effects may not be important for these

very high damping conditions, and simpler lumped parameter models may be used. Alternatively multiple TLM models can be connected in series to represent very high values of β.

The number of weighting terms k can be set according to the required accuracy and the bandwidth of the pressure and flow pulsations. For the step responses considered in this paper, where the pulsation frequency and shape is governed by the pipeline length and damping, five or six terms is generally enough and little or no improvement in the results is gained by using more than six terms. The parameters for the model with six terms are presented here in Appendix 2, so it is not necessary to perform the optimisation process again in order to use the model.

The TLM model has been applied to a switched inertance hydraulic system. It has proved to be very effective in this situation and enabled an efficient, robust and accurate system model. However it is difficult to judge the TLM model to a high degree of accuracy by comparing with experimental results, as discrepancies tend to be introduced by uncertainties in the experimental boundary conditions or limitations in the modelling of the boundary conditions. It is considered to be more useful and meaningful to compare the numerical model with the well-established and precise analytical model, as has been done in this paper.

The TLM model could very usefully be extended to turbulent flow. However this is more complex as additional factors need to be considered – Reynolds number and roughness. The flowrate history also needs to be considered as the turbulence parameters do not change instantaneously with Reynolds number [18, 19]. A preliminary investigation has been done using the previous TLM model and this gave encouraging results, subject to the known accuracy limitations of that model. It will be significantly more difficult to develop the new model for turbulent flow, and this

may necessitate another dimension in the lookup tables unless simplifications can be made. It may also require that the coefficients are time-dependent as Reynolds number will change during a transient simulation.

6. Conclusions

Existing transmission line models have been found to be inaccurate under certain circumstances. The reasons for these inaccuracies have been analysed. A new TLM model has been developed to enhance the transient and steady state accuracy, with the result that very good agreement is obtained between the TLM and an analytical model. However the enhanced model is slightly more complicated, and the previous model [10] may be sufficiently accurate for many applications.

The TLM has been implemented in Matlab Simulink and is available for downloading [20]. It has been used in various system models and has been found to be reliable and efficient. It is easy to link into system simulations using variable time step solvers. However at present it is limited to laminar flow with linear, time-invariant properties.

Acknowledgment

This work was supported by the UK Engineering and Physical Sciences Research Council under grant number EP/H024190/1, together with Instron, JCB and Parker Hannifin. Their support is greatly appreciated.

References

[1] Mathworks product documentation: segmented pipeline, http://www.mathworks.it/help/toolbox/physmod/hydro/ref/segmentedpipeline.html, accessed June 2011

[2] Vitkovsky, J., Lambert, M., Simpson, A. and Bergant, A., Advances in unsteady friction modelling in transient pipe flow, BHR Group conference on Pressure Surges, Safe Design and Operation of Industrial Pipe Systems, BHR Group Conf. Series, Pub. No. 39, 2000

[3] Wylie, E.B, *Fluid Transients*, revised edition, New York & London, McGraw Hill, 1978

[4] Taylor, S. E. M., Johnston, D. N. and Longmore, D. K., Modelling of transient flows in hydraulic pipelines, Proc. IMechE Pt I, vol. 211, no. I6, 1997, 447-456

[5] Watton, J. and Tadmori, M.J. A comparison of techniques for the analysis of transmission line dynamics in electrohydraulic control systems. Applied Mathematical Modelling, vol. 12, Oct. 1988, 457-466.

[6] Wongputorn, W., Hullender, D.A., and Woods, R.L. Rational Polynomial Transfer Function Approximations for Fluid Transients in Lines, Proc. of ASME FEDSM'03, 4th ASME_JSME Joint Fluids Engineering Conference, FEDSM2003-45247, Honolulu, Hawaii, July 2003

[7] Karam, J.T. and Leonard, R.G., A simple yet theoretically based time domain model for fluid transmission line systems, Trans. ASME, Journal of Fluids Engineering, Vol. 95, Series I, No. 4, Dec 1973, pp498-504

[8] Krus, P., Weddfelt, K. and Palmberg, J-O., Fast pipeline models for simulation of hydraulic systems, Journal of Dynamic Systems, Measurement and Control, Trans. ASME, v 116, no. 1, Mar, 1994, 132-136

[9] Johnston, D. N., Efficient methods for numerical modeling of laminar friction in fluid lines, Trans. ASME, Journal of Dynamic Systems Measurement and Control Vol. 128, No. 4, Dec. 2006, pp829-834

[10] Johnston, D.N., The Transmission Line Method for Modelling Laminar Flow of Liquid in Pipelines, Proc IMechE Part I, 2012 226: 586-597, May 2012

[11] Burton J.D., Edge K.A. and Burrows CR, Modeling requirements for the parallel simulation of hydraulic systems, Journal of Dynamic Systems, Measurement and Control, vol. 116, 1994, pp137-145

[12] Axin, M., Braun, R., Dell'Amico, A., Eriksson, B., Nordin, P., Petterson, K., Staak, I and Krus, P. Next generation simulation software using transmission line elements, Proceedings of Bath/ASME Symposium on Fluid Power and Motion Control 2010, Bath, 15-17 September 2010, University of Bath

[13] Scheidl, R., Manhartsgruber, B and Winkler, B., "Hydraulic switching control – principles and state of the art," The First Workshop on Digital Fluid Power, Tampere, Finland, 2008.

[14] Johnston, D.N., A Switched Inertance device for Efficient Control of Pressure and Flow, Bath/ASME Symposium on Fluid Power and Motion Control, Hollywood, October 2009

[15] Goodson, R.E. and Leonard, R.G. A Survey of Modeling Techniques for Fluid Line Transients, Trans. ASME, Jour. Basic Eng., June 1972, p474

[16] Stecki, J.S. and Davis, D.C. Fluid transmission lines-distributed parameter models. Part 1: a review of the state of the art. Proc IMechE, vol. 200, no. A4, 1986, 215-228.

[17] Pan, M., Johnston, D.N, Plummer, A.R., Kudzma, S., Hillis, A.J., Theoretical and experimental studies of a switched inertance hydraulic system, Proc IMechE, Part I, 2013

[18] Brown, F.T., Margolis, D.L. and Shah, R.P., Small Amplitude Frequency Behavior of Fluid Lines with Turbulent Flow, Journal of Basic Eng., Trans. ASME, December, 1969, pp678-692

[19] Johnston, D.N., Numerical modelling of unsteady turbulent flow in tubes, including the effects of roughness and large changes in Reynolds number, Proceedings of the Institution of Mechanical Engineers, Part C: Journal of Mechanical Engineering Science August 2011 225: 1874-1885

[20] Johnston, D.N., Pipeline models in Matlab Simulink, available from http://people.bath.ac.uk/ensdnj/models, accessed July 2013

Appendix 1: Nomenclature

A	Internal cross-sectional area
c	Speed of sound
C_1, C_2	Characteristic at end 1 and 2
E	Weighting function
F	Weighting function
G	Weighting function
G_1	Steady friction component of G
G_2	Unsteady friction component of G
H	Friction function
J_0, J_1, J_2	Bessel functions of the first kind
L	Length of pipeline
m_i	Coefficient of weighting function
m_{Ei}	Coefficient of weighting function for E
m_{Gi}	Coefficient of weighting function for G
n_i	Coefficient of weighting function
N	Friction function
r	Internal radius of pipe
R	Resistance
p_1, p_2	Pressure at end 1 and 2
P_1, P_2	Fourier transform of pressure at end 1 and 2
q_1, q_2	Flow into end 1 and 2
Q_1, Q_2	Fourier transform of flow into end 1 and 2
$t_{11}, t_{12}, t_{21}, t_{22}$	Analytical transmission matrix terms
$t_{11}^*, t_{12}^*, t_{21}^*, t_{22}^*$	Modelled transmission matrix terms
T	Wave propagation time for pipeline
T'	Adjusted delay time for model
V	Fluid volume in pipeline
z	Complex non-dimensional frequency parameter
Z_C	Characteristic impedance
Δp	Pressure difference across ends of pipe
Δq	Magnitude of step change in flowrate
ΔV	Volume of fluid injected into pipe
α	Non-dimensional frequency
β	Dissipation number
ε	Error
κ	Empirical factor
λ	Wavelength
ν	Kinematic viscosity
ρ	Fluid density
ω	Angular frequency

Appendix 2: Tables of weights for 6-term series

Table 3 Weights for E

β	m_{E1}	m_{E2}	m_{E3}	m_{E4}	m_{E5}	m_{E6}
0.0001	0.005224	0.00028	0.001957	0.006269	0.01886	0.05642
0.000133	0.006014	0.000357	0.00229	0.00729	0.02193	0.065632
0.000178	0.006918	0.000457	0.002684	0.008489	0.025523	0.076406
0.000237	0.00795	0.000587	0.003154	0.009898	0.029735	0.089023
0.000316	0.009123	0.000759	0.003715	0.011559	0.034678	0.103822
0.000422	0.01043	0.001004	0.004503	0.013911	0.041724	0.112346
0.000562	0.011873	0.001345	0.005576	0.017134	0.051391	0.112413
0.00075	0.013448	0.001815	0.006984	0.021346	0.064019	0.103591
0.001	0.015139	0.002459	0.008842	0.026882	0.080616	0.080978
0.001334	0.016918	0.003334	0.011288	0.034145	0.102377	0.038864
0.001778	0.01872	0.0046	0.0148	0.04452	0.085382	0.088978
0.002371	0.020433	0.006384	0.019861	0.059608	0.051	0.152626
0.003162	0.021541	0.009762	0.029582	0.050599	0.067159	0.201189
0.004217	0.022063	0.014855	0.042392	0.031041	0.092996	0.278335
0.005623	0.020802	0.026993	0.040999	0.044018	0.105609	0.316673
0.007499	0.01905	0.039761	0.045404	0.053708	0.118626	0.35557
0.01	0.018107	0.049415	0.064419	0.045936	0.137568	0.412546
0.013335	0.017792	0.058637	0.08845	0.048627	0.145573	0.436719
0.017783	0.022452	0.062431	0.120783	0.050613	0.151709	0.455088
0.023714	0.033358	0.064688	0.150064	0.055224	0.165602	0.496748
0.031623	0.049046	0.070715	0.171912	0.063309	0.189932	0.569684
0.04217	0.065722	0.090133	0.18034	0.075641	0.226946	0.680707
0.056234	0.080943	0.130838	0.172406	0.091602	0.274813	0.824296
0.074989	0.094505	0.195053	0.155481	0.107548	0.322683	0.967929
0.1	0.107712	0.281616	0.141863	0.11916	0.357638	1.0729
0.133352	0.123113	0.389289	0.136899	0.126441	0.379639	1.13897
0.177828	0.144203	0.519871	0.127579	0.138422	0.415811	1.24755
0.237137	0.178576	0.670638	0.093133	0.168379	0.505848	1.51776
0.316228	0.229176	0.831103	0.090869	0.224069	0.521304	1.56407
0.421697	0.318762	0.935833	0.177905	0.540387	0.232797	0.698746
0.562341	0.476083	0.947676	0.27107	0.827213	0.170571	0.513138
0.749894	0.643645	1.00269	0.510308	0.512483	0.529807	1.6152
1	0.593385	1.24543	0.938237	0.762194	2.51601	7.89072

Table 4 Weights for G and τ

β	m_{G1}	m_{G2}	m_{G3}	m_{G4}	m_{G5}	m_{G6}	τ
0.0001	0.005281	0	0.000752	0.01526	0	0.043497	1.00047
0.000133	0.006072	0	0.001095	0.017373	0	0.050316	1.00054
0.000178	0.006976	0	0.001567	0.019727	0	0.058228	1.00062
0.000237	0.008004	0	0.002217	0.022329	0	0.067422	1.00072
0.000316	0.009168	0	0.003108	0.02517	1.68E-05	0.078096	1.00082
0.000422	0.010465	0	0.004568	0.027162	0.002838	0.085756	1.00098
0.000562	0.011896	0	0.006654	0.028678	0.007242	0.092952	1.00117
0.00075	0.013456	0	0.009568	0.02945	0.013743	0.099223	1.00141
0.001	0.015126	0	0.013597	0.029073	0.023083	0.103854	1.0017
0.001334	0.016881	0	0.019075	0.027091	0.036102	0.106014	1.00206
0.001778	0.018675	0	0.026489	0.022941	0.053319	0.10429	1.00252
0.002371	0.020324	0.000654	0.034608	0.018856	0.072203	0.102424	1.00304
0.003162	0.020886	0.006192	0.03379	0.029262	0.074279	0.124191	1.00341
0.004217	0.020793	0.01381	0.031767	0.042678	0.074396	0.150901	1.00379
0.005623	0.019354	0.02491	0.027194	0.060007	0.074838	0.178772	1.00421
0.007499	0.017404	0.036458	0.025483	0.076106	0.079963	0.202558	1.00473
0.01	0.016047	0.045638	0.031119	0.086445	0.09429	0.215674	1.00545
0.013335	0.015258	0.053672	0.040232	0.098934	0.108665	0.229636	1.0062
0.017783	0.018798	0.056843	0.055246	0.109522	0.127279	0.237375	1.00706
0.023714	0.027864	0.057489	0.07057	0.122702	0.144791	0.245414	1.00792
0.031623	0.041049	0.059954	0.081052	0.143575	0.156545	0.25909	1.00859
0.04217	0.055185	0.070266	0.082903	0.174329	0.162444	0.278455	1.0088
0.056234	0.068417	0.092116	0.077021	0.211043	0.169426	0.299161	1.00798
0.074989	0.08059	0.125688	0.069245	0.242871	0.190806	0.287179	1.00666
0.1	0.092371	0.170209	0.062699	0.261616	0.206408	0.206439	1.0098
0.133352	0.105223	0.226105	0.057112	0.270498	0.212392	0.128658	1.01335
0.177828	0.121249	0.294258	0.048478	0.266598	0.209589	0.059833	1.01704
0.237137	0.145048	0.374495	0.026291	0.254982	0.19425	0.004997	1.02071
0.316228	0.182775	0.445286	0.00886	0.252796	0.110269	0	1.02825
0.421697	0.250535	0.479733	0.007109	0.228974	0.033674	0	1.03608
0.562341	0.363395	0.474821	0	0.161637	0	0	1.04608
0.749894	0.478032	0.460853	0	0.060783	0	0	1.06002
1	0.5	0.470745	0.029126	0	0	0	1.07869